





# Analysis of critical imposed load of plate using variational calculus

Festus C. Onyeka <sup>a,\*</sup>, Thompson E. Okeke <sup>b</sup>

<sup>a</sup> Department of Civil Engineering, Edo University Iyamho, Edo State, Nigeria

<sup>b</sup> Department of Civil Engineering, University of Nigeria, Nsukka, Enugu State, Nigeria

## ARTICLE INFO

### Article history:

Received 12 September 2020

Received in revised form  
1 October 2020

Accepted 20 October 2020

Available online  
24 October 2020

### Keywords:

CCFS plate

Critical lateral imposed load

Elastic yielding point

Shear deformation plate  
theory

## ABSTRACT

This work studied the critical load analysis of rectangular plates, carrying uniformly distributed loads utilizing direct variational energy calculus. The aim of this study is to establish the techniques for calculating the critical lateral imposed loads of the plate before deflection attains the specified maximum threshold,  $q_{iw}$  as well as its corresponding critical lateral imposed load before the plate reaches an elastic yield point  $q_{ip}$ . The formulated potential energy by the static elastic theory of the plate was minimized to get the shear deformation and coefficient of deflection. The plates under consideration are clamped at the first and second edges, free of support at the third edge and simply supported at the fourth edge (CCFS). From the numerical analysis obtained, it is found that the critical lateral imposed loads ( $q_{iw}$  and  $q_{ip}$ ) increase as the thickness ( $t$ ) of plate increases, and decrease as the length to width ratio increases. This suggests that as the thickness increases, the allowable deflection improves the safety of the plate, whereas an increase in the span (length) of the plate increases the failure tendency of the plate structure.

## 1. Introduction

Plates have wide applications in floor slabs for buildings, flat panels for aircrafts and bridge decks [1]. Relying on the linear strain–displacement methods for non-linear stress and bending analysis is proven to adversely affect the strength and deflection of plates [2]. This becomes one of the greatest bending and even stability problems with the plate structures. Nevertheless, the object of the solution is to find the smallest load that causes deflection in the plate by developing a non-linear strain–displacement expressions. This smallest load can be said to be critical

because the critical load puts the plate in a state of unstable equilibrium.

As a result of rising usage of plate in engineering, the need for the advanced approach become easily exposed. Some cases of plate material, transverse strains and stresses influence the flexural characteristics very much. There is a need to develop the displacement model that will assume care of effect of transverse shear stress so as to generate a reliable formulation of whatever type of plate at given boundary condition [3]–[7].

Isotropic plates are being extensively utilized in structures that are subjected to severe uniformly distributed loads that bring

\* Corresponding author

E-mail address: [onyeka.festus@edouniversity.edu.ng](mailto:onyeka.festus@edouniversity.edu.ng)  
<https://doi.org/10.37121/jase.v4i1.125>

out relatively great stresses on it. In order to evaluate the actual load in the plate when large stresses characterized by non-negligible shear deformations, refined theories are developed [8]-[12]. Results established by applying the trigonometric, exponential and hyperbolic shear deformation theories show inconsiderable fluff in estimating reactions of lateral loads on the structures as a result of wearisome whatness and uncertainty of works involving the application of Fourier series in the thick plate analysis.

In [13], the authors applied polynomial shear deformation theory (PSDT) in analyzing isotropic thick plate. The stress solution deduced is devoid of analytical fluff, but did not consider critical lateral loads in anticipating responses of applied loads that could lead to failure on the structures. In [14], PSDT was utilized for the analysis of critical lateral loads in anticipating responses of applied loads for rectangular thick plates. These studies [13], [14] neither checked for the effect of shear stress, nor worked for other boundary conditions.

In this study, the bending analysis of rectangular plates, carrying uniformly distributed loads was performed in a thick considering shear deformation effect using the direct variational energy calculus. The formulas for calculating the critical laterally imposed loads of the plate were found out and used to solve bending problem of plate clamped at two edges, free of support at the other edge and simply supported at the remaining edge (CCFS). This will check the deflection and shear in the plate.

## 2. Methodology

### 2.1. Kinematics and Constitutive Relations

The deflection and in-plane displacement functions ( $w$ ,  $v$  and  $u$ ) of the plate were obtained from the displacement-strain relations and stress-strain relations. Taking a rectangular plate subjected to a uniformly distributed load as shown in Fig. 1, the corresponding relationship was demonstrated by applying hooks law.

The in-plane displacement components along x-axis ( $u$ ) and in-plane displacement components along y-axis ( $v$ ) are presented in equations (1) and (2) respectively:

$$u = \frac{zdw}{dy} + F.\theta_{sx}; \quad (1)$$

$$v = \frac{zdw}{dy} + F.\theta_{sy}; \quad (2)$$

given that,  $F = F(z)$  and  $w = w(x, y)$ .

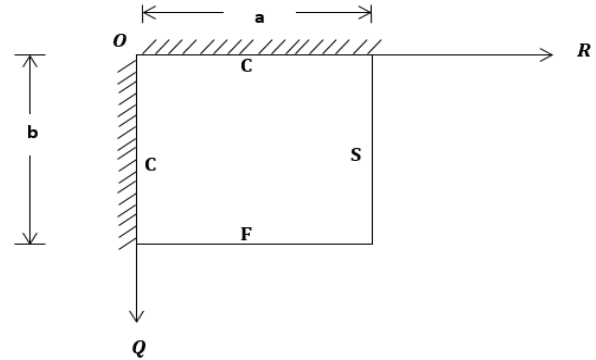


**Fig. 1** CCFS Rectangular plate subjected to a uniformly distributed load.

Substituting appropriately (see [14]) gives the following equations:

$$\sigma_x = \frac{E \left[ \left( -\frac{zd^2w}{dx^2} + \frac{Fd\theta_{sx}}{dx} \right) - \mu \left( \frac{zd^2w}{dy^2} + \frac{Fd\theta_{sy}}{dy} \right) \right]}{(1-\mu^2)} \quad (3)$$

$$\sigma_y = \frac{E \left[ \left( -\frac{zd^2w}{dy^2} + \frac{Fd\theta_{sy}}{dy} \right) - \mu \left( \frac{zd^2w}{dx^2} + \frac{Fd\theta_{sx}}{dx} \right) \right]}{(1-\mu^2)} \quad (4)$$

$$\tau_{xy} = 2G \left[ -\frac{zd^2w}{\partial x \partial y} + F \left( \frac{d\theta_{sx}}{dy} + \frac{d\theta_{sy}}{dx} \right) \right] \quad (5)$$

$$\tau_{xz} = 2G \left[ \frac{zd^2w}{\partial x \partial z} + F \left( \frac{d\theta_{sx}}{dz} + \frac{d\theta_{sz}}{dx} \right) \right] \quad (6)$$

$$\tau_{yz} = 2G \left[ \frac{zd^2w}{\partial y \partial z} + F \left( \frac{d\theta_{sy}}{dz} + \frac{d\theta_{sz}}{dy} \right) \right] \quad (7)$$

As described in [14]:

$$G = \frac{E(1-\mu)}{2(1-\mu^2)} \quad (8)$$

$$F(z) = \frac{3}{2} \left( z - \frac{4z^3}{3t^2} \right) \quad (9)$$

The symbol  $w$  denotes deflection,  $F(z)$  denotes shear deformation profile,  $\theta_{sx}$  and  $\theta_{sy}$  denotes shear deformation rotation along x-axis and y-axis, respectively;  $\mu$  denotes poisson ratio,  $E$  denotes modulus of elasticity of the plate,  $\sigma_x$  and  $\sigma_y$  denotes stress normal to the x-axis and y-axis, respectively; and  $\tau_{xy}$ ,  $\tau_{xz}$  and  $\tau_{yz}$  denotes shear stress along x-y, x-z and y-z axis, respectively.

### 2.2. The Total Potential Energy Equation

The total potential energy ( $\Pi$ ) of a plate is given as [13]:

$$\Pi = U + V, \quad (10)$$

given that  $U$  and  $V$  are the strain energy and external work respectively; expressed in equations (11) and (12); where,  $q$  is the uniformly distributed load,  $\varepsilon_x$  and  $\varepsilon_y$  denotes normal strain along x-axis and y-axis, respectively; and  $\gamma_{xy}$ ,  $\gamma_{xz}$  and  $\gamma_{yz}$  denotes shear strain along x-y, x-z and y-z axis, respectively. Thus, the total potential energy of a plate is given in equation (13).

$$V = - \int_0^a \int_0^b qw(x,y) \partial x \partial y, \tag{11}$$

$$U = \frac{1}{2} \iiint_{-\frac{t}{2}}^{\frac{t}{2}} (\sigma_x \epsilon_x + \sigma_y \epsilon_y + \tau_{xy} \gamma_{xy} + \tau_{xz} \gamma_{xz} + \tau_{yz} \gamma_{yz}) dx dy dz, \tag{12}$$

$$\begin{aligned} \Pi = \frac{D}{2} \int_0^a \int_0^b & \left[ \left| g_1 \left( \frac{\partial^2 w}{\partial x^2} \right)^2 - 2g_2 \left( \frac{\partial^2 w}{\partial x^2} \cdot \frac{\partial \theta_{Sx}}{\partial x} \right) + g_3 \left( \frac{\partial \theta_{Sx}}{\partial x} \right)^2 \right| + \left| 2g_1 \left( \frac{\partial^2 w}{\partial x \partial y} \right)^2 - 2g_2 \left( \frac{\partial^2 w}{\partial x \partial y} \cdot \frac{\partial \theta_{Sx}}{\partial y} \right) \right. \right. \\ & \left. \left. - 2g_2 \left( \frac{\partial^2 w}{\partial x \partial y} \cdot \frac{\partial \theta_{Sy}}{\partial x} \right) \right| + \left| (1 + \mu) g_3 \left( \frac{\partial \theta_{Sx}}{\partial y} \right) \left( \frac{\partial \theta_{Sy}}{\partial x} \right) \right| + \frac{(1-\mu)}{2} \left| g_3 \left( \frac{\partial \theta_{Sx}}{\partial y} \right)^2 + g_3 \left( \frac{\partial \theta_{Sy}}{\partial x} \right)^2 \right| \right. \\ & \left. + \left| g_1 \left( \frac{\partial^2 w}{\partial y^2} \right)^2 - 2g_2 \left( \frac{\partial^2 w}{\partial y^2} \cdot \frac{\partial \theta_{Sy}}{\partial y} \right) + g_3 \left( \frac{\partial \theta_{Sy}}{\partial y} \right)^2 \right| + \left| \frac{(1-\mu)}{2} g_4 (\theta_{Sx})^2 + \frac{(1-\mu)}{2} g_4 (\theta_{Sy})^2 \right| \right] \partial x \partial y \\ & - \int_0^a \int_0^b qw(x,y) \partial x \partial y. \tag{13} \end{aligned}$$

Where;

$$g_1 = \left( \frac{t^3}{12} \right) \cdot \left( \frac{12}{t^3} \right) \equiv 1, \tag{14a}$$

$$g_2 = 1.5 \cdot \left( \frac{12}{15} \right) \equiv 1.2, \tag{14b}$$

$$g_3 = 1.5 \cdot \left( 1 - \frac{3}{27} \right) \equiv 1.33, \tag{14c}$$

$$g_4 = \left( 1.5 \left( \frac{d \left( \frac{3t^2z - 4z^3}{3t^2} \right)}{dz} \right)^2 \right)^{\frac{t}{2}} \cdot \left( \frac{12}{t^3} \right) = 14.4, \tag{14d}$$

and the rigidity,  $D$  is defined as:

$$D = \frac{Et^3}{12(1-\mu^2)}. \tag{14e}$$

### 2.3. Governing Energy Equation

*General governing equation:* Differentiating the total potential energy equation (13) with respect to  $w$ ,  $\theta_{Sx}$  and  $\theta_{Sy}$ , gives:

$$\frac{\partial \Pi}{\partial w} = \frac{\partial \Pi}{\partial \theta_{Sx}} = \frac{\partial \Pi}{\partial \theta_{Sy}} = 0. \tag{15}$$

Thus:

$$w = \left( a_0 + a_1 R + \frac{a_2 R^2}{2} + \frac{a_3 R^3}{6} + \frac{qa^4}{D} \left( \frac{n_1}{w_3} \right) \cdot \frac{R^4}{24} \right) \times \left( b_0 + b_1 Q + \frac{b_2 Q^2}{2} + \frac{b_3 Q^3}{6} + \frac{qa^4}{D} \left( \frac{n_1}{w_3} \right) \cdot \frac{Q^4}{24} \right). \tag{16}$$

Similarly;

$$\theta_{Sx} = \left( a_4 + a_5 R + \frac{a_6 R^2}{2} + \frac{qa^3}{D} \left( \frac{n_4}{g_2 \theta_3} \right) \cdot \frac{R^3}{6} \right) \times \left( b_7 + b_8 Q + \frac{b_9 Q^2}{2} + \frac{b_{10} Q^3}{6} + \frac{b_{11} Q^4}{24} \right), \tag{17}$$

$$\theta_{Sy} = \left( a_7 + a_8 R + \frac{a_9 R^2}{2} + \frac{a_{10} R^3}{6} + \frac{a_{11} R^4}{24} \right) \times \left( b_4 + b_5 Q + \frac{b_6 Q^2}{2} + \frac{qa^3}{D} \left( \frac{\alpha^3 n_5}{g_2 \theta_1} \right) \cdot \frac{Q^3}{6} \right). \tag{18}$$

Now, consider the plate in Fig. 1 for numerical analysis; when equation (13) is subjected to boundary conditions of the plate in the Fig. 1, the actual deflection of the plate becomes:

$$w = \frac{F_{a4} \cdot b_5}{17280} (R^2 - 2R^3 + R^4) \times (2.8Q^2 - 5.2Q^3 + 3.8Q^4 - Q^5); \tag{19}$$

amplitude,  $A_s$  and shape function,  $h$  are given as shown in equations (20) and (21), respectively.

$$A_s = \frac{F_{a4} \cdot b_5}{17280}. \tag{20}$$

$$h = (R^2 - 2R^3 + R^4) \times (2.8Q^2 - 5.2Q^3 + 3.8Q^4 - Q^5). \tag{21}$$

Therefore:

$$k_1 = \int_0^1 \int_0^1 \left( \frac{d^2 h}{dR^2} \right)^2 dR dQ \tag{22}$$

$$k_2 = \int_0^1 \int_0^1 \left( \frac{d^2 h}{dR dQ} \right)^2 dR dQ \tag{23}$$

$$k_3 = \int_0^1 \int_0^1 \left( \frac{d^2 h}{dQ^2} \right)^2 dR dQ \tag{24}$$

$$k_4 = \int_0^1 \int_0^1 \left( \frac{dh}{dR} \right)^2 dR dQ \tag{25}$$

$$k_5 = \int_0^1 \int_0^1 \left( \frac{dh}{dQ} \right)^2 dR dQ \tag{26}$$

$$k_q = \int_0^1 \int_0^1 h \cdot dR dQ \tag{27}$$

The values of stiffness coefficient ( $k_1, k_2, k_3, k_4, k_5$  and  $k_q$ ) obtained from equations (22) to (27) are presented in Table 1.

**Table 1** Values of stiffness coefficient,  $k$  for various support.

Type	Plate	$k_1$	$k_2$	$k_3$	$k_4$	$k_5$	$k_q$
1	CCFS	0.1231792	0.0162176	0.0197152	0.0058657	0.00142656	0.017

**Direct governing equation:** The direct variational technique is utilized to obtain the direct governing differential equation by differentiating the total potential energy with respect to the coefficient of deflection  $A_s$ , coefficient of shear deformation with respect to x-axis,  $A_x$  and coefficient of shear deformation with respect to y-axis,  $A_y$ .

The non-dimensional values of quantities along the x- and y-axis respectively is presented as follows, let:

$$x = aR \text{ and } y = bQ \quad (28)$$

The length to breath aspect ratio is:

$$\alpha = \frac{b}{a}; \quad (29)$$

and the span to thickness ratio is:

$$\rho = \frac{a}{t}. \quad (30)$$

The deflection,  $w$  is the product of shape function of the plate and deflection coefficient, expressed as:

$$w = h.A_s. \quad (31)$$

$A_s$  is the coefficient of deflection and  $h$  being the plate shape function.

The shear deformation rotation along the x-axis and y-axis, respectively become:

$$\theta_{Sx} = \left[ \frac{dh}{dR} \right] [A_x]. \quad (32)$$

$$\theta_{Sy} = \left[ \frac{dh}{dQ} \right] [A_y]. \quad (33)$$

Given  $A_x$  and  $A_y$  are the shear deformation along x- and y- axis respectively. By substituting equations (28) to (33) into equation (13), gives equation (34).

$$\begin{aligned} \Pi = & \frac{Et^3}{24(1-\mu^2)a^4} \int_0^1 \int_0^1 \left[ g_1 A_s^2 \left( \frac{\partial^2 h}{\partial R^2} \right)^2 - 2g_2 A_s A_x \left( \frac{\partial^2 h}{\partial R^2} \right)^2 \right. \\ & + g_3 A_x^2 \left( \frac{\partial^2 h}{\partial R^2} \right)^2 + \left. 2g_1 \frac{A_s^2}{\alpha^2} \left( \frac{\partial^2 h}{\partial R \partial Q} \right)^2 - 2g_2 \frac{A_s A_x}{\alpha^2} \left( \frac{\partial^2 h}{\partial R \partial Q} \right)^2 \right. \\ & - 2g_2 \frac{A_s A_y}{\alpha^2} \left( \frac{\partial^2 h}{\partial R \partial Q} \right)^2 \left. + \left( (1+\mu) g_3 \frac{A_x A_y}{\alpha^2} \left( \frac{\partial^2 h}{\partial R \partial Q} \right)^2 + \frac{(1-\mu)}{2} \right. \right. \\ & \times \left. \left. \left| g_3 \frac{A_x^2}{\alpha^2} \left( \frac{\partial^2 h}{\partial R \partial Q} \right)^2 + g_3 \frac{A_y^2}{\alpha^2} \left( \frac{\partial^2 h}{\partial R \partial Q} \right)^2 \right| + \left| g_1 \frac{A_s^2}{\alpha^4} \left( \frac{\partial^2 h}{\partial Q^2} \right)^2 \right. \right. \\ & \left. \left. - 2g_2 \frac{A_s A_y}{\alpha^4} \left( \frac{\partial^2 h}{\partial Q^2} \right)^2 + g_3 \frac{A_y^2}{\alpha^4} \left( \frac{\partial^2 h}{\partial Q^2} \right)^2 \right| + \frac{(1-\mu)}{2} \rho^2 g_4 \times \right. \\ & \left. A_x^2 \left( \frac{\partial h}{\partial R} \right)^2 + \frac{(1-\mu)}{2} \cdot \frac{\rho^2 g_4 A_y^2}{\alpha^2} \left( \frac{\partial h}{\partial Q} \right)^2 \right] ab \partial R \partial Q - \\ & \int_0^1 \int_0^1 q A_s h ab \partial R \partial Q. \quad (34) \end{aligned}$$

Thus:

$$\frac{\partial \Pi}{\partial A_s} = \frac{\partial \Pi}{\partial A_x} = \frac{\partial \Pi}{\partial A_y} = 0; \quad (35)$$

gives:

$$\begin{bmatrix} r_{11} & r_{12} & r_{13} \\ r_{21} & r_{22} & r_{23} \\ r_{31} & r_{32} & r_{33} \end{bmatrix} \begin{bmatrix} A_s \\ A_x \\ A_y \end{bmatrix} = \frac{qa^4}{D} \begin{bmatrix} k_q \\ 0 \\ 0 \end{bmatrix}. \quad (36)$$

Let:

$$r_{11} = g_1 \left( k_1 + \frac{2}{\alpha^2} k_2 + \frac{1}{\alpha^4} k_3 \right). \quad (37)$$

$$r_{12} = -g_2 \left( k_1 + \frac{1}{\alpha^2} k_2 \right). \quad (38)$$

$$r_{13} = -g_2 \left( \frac{1}{\alpha^2} k_2 + \frac{1}{\alpha^4} k_3 \right). \quad (39)$$

$$r_{21} = -g_2 \left( k_1 + \frac{1}{\alpha^2} k_2 \right). \quad (40)$$

$$r_{22} = \left( g_3 k_1 + \frac{(1-\mu)}{2\alpha^2} g_3 k_2 + \frac{(1-\mu)}{2} \rho^2 g_4 k_4 \right). \quad (41)$$

$$r_{23} = g_3 \frac{(1+\mu)}{2\alpha^2} k_2. \quad (42)$$

$$r_{31} = -g_2 \left( \frac{1}{\alpha^2} k_2 + \frac{1}{\alpha^4} k_3 \right). \quad (43)$$

$$r_{32} = g_3 \frac{(1+\mu)}{2\alpha^2} k_2. \quad (44)$$

$$r_{33} = \left( g_3 \frac{(1-\mu)}{2} \left( \frac{1}{\alpha^2} k_2 + \frac{1}{\alpha^4} k_3 \right) + g_4 \frac{(1-\mu)}{2\alpha^2} \rho^2 k_5 \right). \quad (45)$$

$$T_2 = \frac{r_{21} \cdot r_{33} - r_{23} \cdot r_{31}}{r_{22} \cdot r_{33} - r_{23} \cdot r_{32}}. \quad (46)$$

$$T_3 = \frac{r_{21} \cdot r_{32} - r_{22} \cdot r_{31}}{r_{23} \cdot r_{32} - r_{22} \cdot r_{33}}. \quad (47)$$

Therefore;

$$A_s = \frac{qa^4}{D} \left( \frac{k_q}{r_{11} T_1 - r_{12} T_2 - r_{13} T_3} \right). \quad (48)$$

That is:

$$A_s = \frac{qa^4}{D} \left( \frac{k_q}{r_{11} - r_{12} T_2 - r_{13} T_3} \right), \quad (49)$$

where;

$$T_1 = 1. \quad (50)$$

Recall;

$$A_s = \frac{qa^4}{D} (k), \quad (51)$$

where;

$$D = \frac{Et^3}{12(1-\mu^2)}, \quad (52)$$

$$k = \frac{k_q}{k_T}, \quad (53)$$

$$k_T = k_1 + \frac{2}{\alpha^2} k_2 + \frac{1}{\alpha^4} k_3. \quad (54)$$

2.4. Formulation of the Critical Lateral Imposed Load in the Rectangular Plate

Formulation of expression for the critical imposed load before deflection reaches specified maximum limit,  $q_{iw}$ : In order to ensure that deflection does not exceed specified maximum limit (see [2]);

$$w = A_s h < w_a \tag{55}$$

Substituting equations (51) – (53) into equation (55), gives:

$$\frac{12(1-\mu^2)qa^4}{Et^3} \cdot \frac{k_q}{k_T} \cdot h < w_a \tag{56}$$

given that  $w_a$  is the allowable deflection.

Let,

$$q = \gamma + q_{iw} \tag{57}$$

this gives:

$$q_{iw} < Et^3 \frac{w_a k_T}{(1-\mu^2)12.k_q.ha^4} - \gamma \tag{58}$$

Given that,  $\gamma$  is the self-weight of the plate,  $q_{iw}$  is the critical imposed load of the plate and  $i$  is the specific thickness.

Formulation of expression for the critical load before plate reaches elastic yield stress,  $q_{ip}$ : In order to ensure that the plate did not yield beyond the elastic yield stress, the critical lateral imposed load determined according to [14]:

$$U = \frac{1}{2} \iiint_{-\frac{t}{2}}^{\frac{t}{2}} \Omega \, dx dy dz; \tag{59}$$

where;

$$\Omega = \sigma_x \varepsilon_x + \sigma_y \varepsilon_y + \tau_{xy} \gamma_{xy} + \tau_{xz} \gamma_{xz} + \tau_{yz} \gamma_{yz} \tag{60}$$

Substituting values of  $\varepsilon_x, \varepsilon_y, \gamma_{xy}, \gamma_{xz}$  and  $\gamma_{yz}$  into equation (60) gives:

$$\Omega = \frac{1}{E} [\sigma_x^2 - \mu\sigma_x\sigma_y - \mu\sigma_x\sigma_y + \sigma_y^2 + 2(1+\mu)\tau_{xy}^2 + 2(1+\mu)\tau_{xz}^2 + 2(1+\mu)\tau_{yz}^2] \tag{61}$$

But;

$$\Omega = \frac{1}{E} [\sigma_x^2 - \mu\sigma_x\sigma_y - \mu\sigma_x\sigma_y + \sigma_y^2 + 2(1+\mu)\tau_{xy}^2 + 2(1+\mu)\tau_{xz}^2 + 2(1+\mu)\tau_{yz}^2] < \Omega_0 \tag{62}$$

$\Omega_0$  is the yielding point of the plate. For a bar,

$$\sigma_x = fy \tag{63}$$

$$\sigma_y = \tau_{xy} = \tau_{xz} = \tau_{yz} = 0 \tag{64}$$

Therefore;

$$\Omega < \Omega_0 > \frac{fy^2}{E} \tag{65}$$

Substituting equation (62) into (65) gives:

$$\frac{1}{E} [\sigma_x^2 - 2\mu\sigma_x\sigma_y + \sigma_y^2 + 2(1+\mu)\tau_{xy}^2 + 2(1+\mu)\tau_{xz}^2 + 2(1+\mu)\tau_{yz}^2] < \frac{fy^2}{E} \tag{66}$$

Let,

$$\sigma_y = n_1\sigma_x \tag{67}$$

$$\tau_{xy} = n_2\sigma_x \tag{68}$$

$$\tau_{xz} = n_3\sigma_x \tag{69}$$

$$\tau_{yz} = n_4\sigma_x \tag{70}$$

Therefore, substituting equations (67) to (70) into equation (66) gives:

$$\sigma_x^2 - 2\mu n_1\sigma_x^2 + n_1^2\sigma_x^2 + 2(1+\mu)n_2^2\sigma_x^2 + 2(1+\mu)n_3^2\sigma_x^2 + 2(1+\mu)n_4^2\sigma_x^2 < fy^2 \tag{71}$$

$$\sigma_x < \frac{fy}{\sqrt{[1-2\mu n_1+n_1^2+2(1+\mu)n_2^2+2(1+\mu)n_3^2+2(1+\mu)n_4^2]}} \tag{72}$$

The value of  $\sigma_x$  according to [14] gives:

$$\sigma_x = \frac{EstA_s}{(1-\mu^2)\alpha^2} \left( \frac{d^2h}{dR^2} + \frac{\mu}{\alpha^2} \frac{d^2h}{dQ^2} \right) \tag{73}$$

Thus:

$$\sigma_x = s \left( \frac{d^2h}{dR^2} + \frac{\mu}{\alpha^2} \frac{d^2h}{dQ^2} \right) \frac{qa^2}{t^2} \cdot 12k \tag{74}$$

Equating equations (72) and (74), gives equation (75):

$$\frac{12.qa^2.k.s}{t^2} \cdot C_2 < \frac{fy}{C_3}; \tag{75}$$

where;

$$\beta_2 = \left( \frac{d^2h}{dR^2} + \frac{\mu}{\alpha^2} \frac{d^2h}{dQ^2} \right) \tag{76}$$

and

$$\beta_3 = \sqrt{[1-2\mu n_1+n_1^2+2(1+\mu)n_2^2+2(1+\mu)n_3^2+2(1+\mu)n_4^2]} \tag{77}$$

Making  $q$ , the subject of expression in equation (75), gives:

$$q < \frac{fyt^2}{12.a^2.k.s.C_2.C_3} \tag{78}$$

Let;

$$q = q_s + q_{ip} \tag{79}$$

This gives:

$$q_{ip} < \frac{fyt^2}{12.a^2.k.s.C_2.C_3} - q_s; \tag{80}$$

$$q_{ip} < \frac{fyt^2}{12.a^2.k.s.C_2.C_3} - \gamma t; \tag{81}$$

$$q_{ip} < \beta_4 t^2 - \gamma t; \tag{82}$$

where;

$$\beta_4 = f_y / 12 \cdot a^2 \cdot \frac{k_q}{k_T} \cdot st \cdot C_2 \cdot C_3, \tag{83}$$

$q_{ip}$  is the critical imposed lateral load before plate reach yield stress,  $f_y$  is the strength,  $i$  is the specific thickness and  $q_a$  is the self-weight of the plate.

### 3. Results and Discussion

Figs. 2 to 4 show the CCFS plate with span of 1000mm at allowable deflection ( $w_a$ ), value

between 1 mm to 5 mm. It is shown that failure neither occurs on  $q_{iw}$  nor  $q_{ip}$  at any thickness and length to width ratio. In the span of 3000 mm as presented in Fig. 5, it is also seen that failure neither occurs on  $q_{iw}$  nor  $q_{ip}$  at any thickness and length to width ratio. It's worth to note that the positive value of the load,  $q_{iw}$  and  $q_{ip}$  shows that the plate neither fail in  $q_{iw}$  nor  $q_{ip}$  for plate all span at specified deflection,  $w_a$  of 1000 mm to 5000 mm. This means that the plate structure is safe.

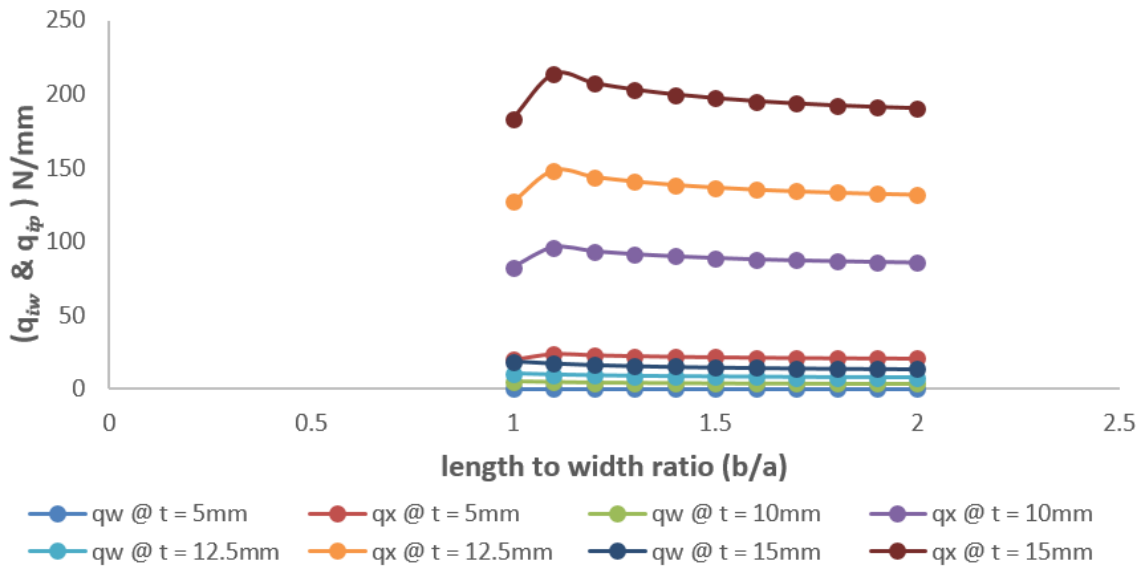


Fig. 2 Graph of critical load versus length to width ratio of CCFS plate for span, a = 1.0 m at  $w_a = 3.0$  mm.

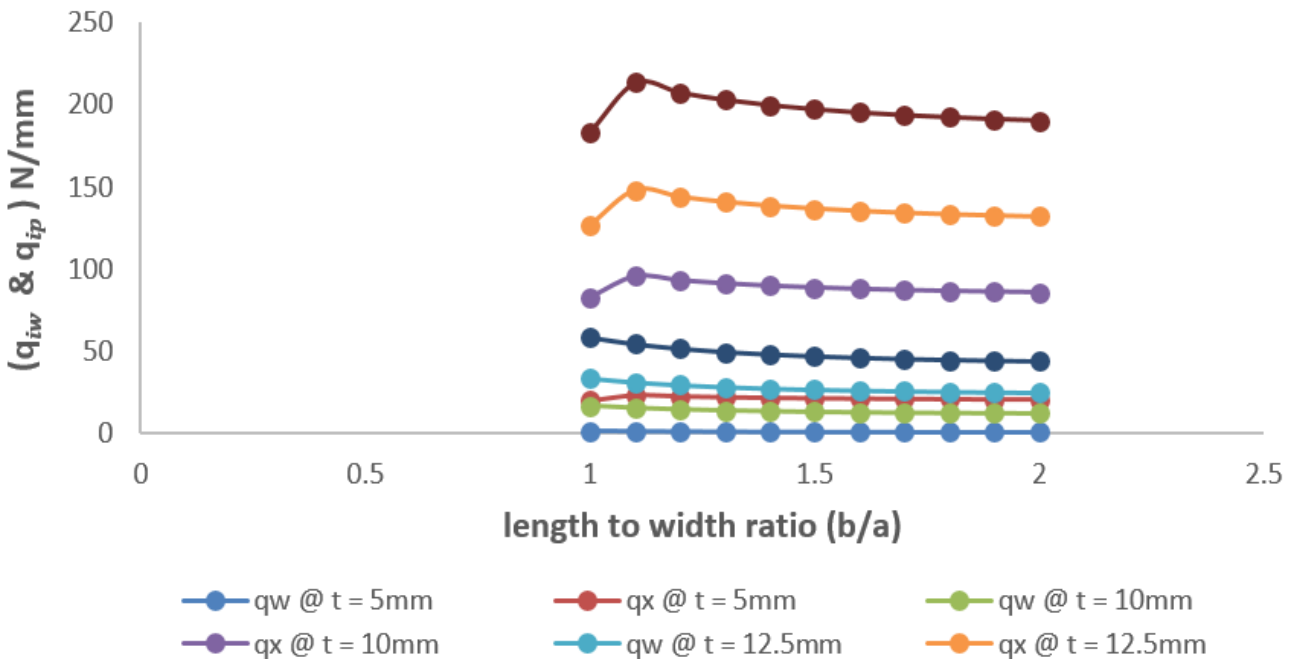
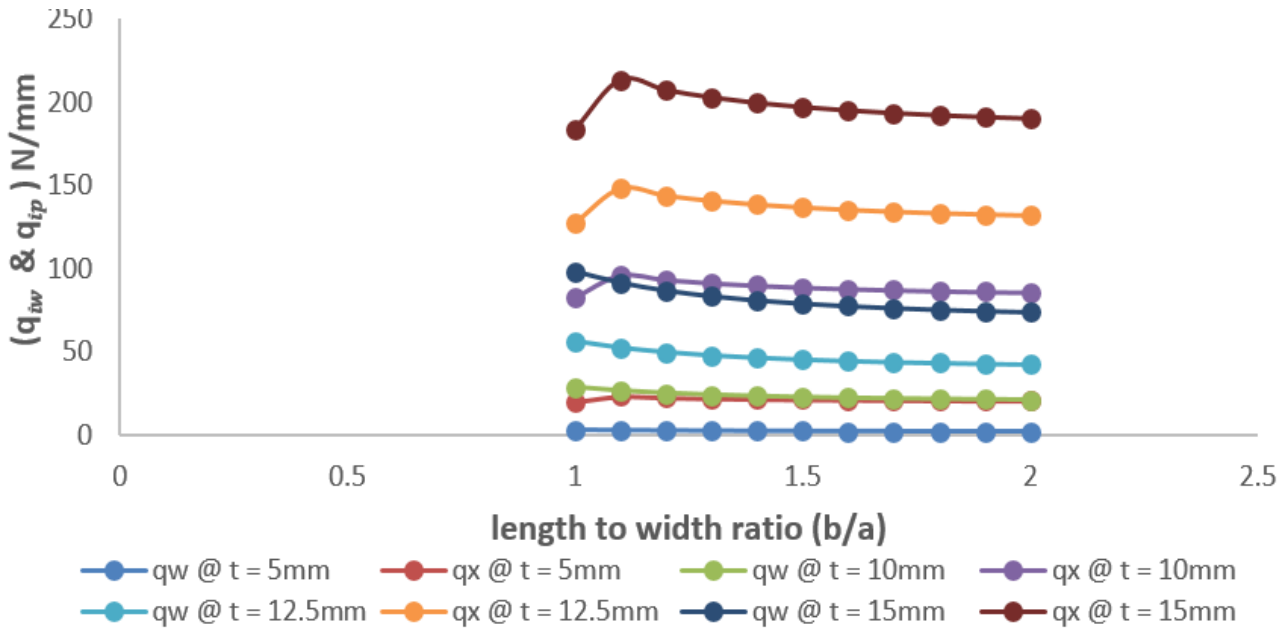
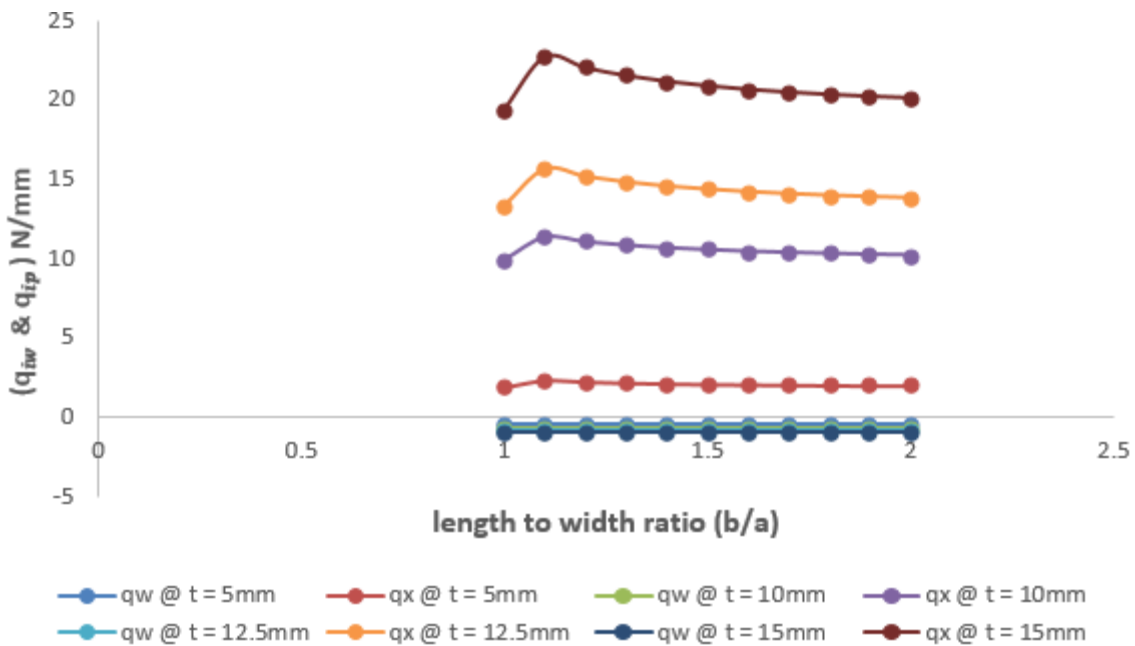


Fig. 3 Graph of critical load versus length to width ratio of CCFS plate for span, a = 1.0 m at  $w_a = 3.0$  mm.



**Fig. 4** Graph of critical load versus length to width ratio of CCFS plate for span, a = 1.0 m at  $w_a = 5.0$  mm.



**Fig. 5** Graph of critical load versus length to width ratio of CCFS plate for span, a = 3.0 m at  $w_a = 3.0$  mm.

Looking closely at Figs. 6 to 10 illustrating the CCFS plate with span between 1000 mm and 5000 mm, at allowable deflection ( $w_a$ ) value between 1 mm and 5 mm. It finds that failure in  $q_{iw}$  only occurs at all length to width ratio (1 to 2) with the highest value of -1.0347 N/mm at all thickness. The negative value of critical lateral imposed load,  $q_{iw}$  (and positive value of  $q_{ip}$ ) only reveals that the plate fails in  $q_{iw}$  for the entire plate,  $w_a$  (5 mm to 15 mm) and a span of 3000 mm to 5000 mm. This means that the plate structure is not safe rather required maintenance.

In summary, failure in deflection ( $q_{iw}$ ) is seen in the CCFS plate, but failure in shear ( $q_{ip}$ ), which leads to crack is not seen in all the aspect ratio in consideration. Furthermore, from the numerical analysis obtained as presented in the Figs. 2 to 10. It is found that the value of critical lateral imposed load ( $q_{iw} & q_{ip}$ ), increase as the specified thickness (t), of plate increases and decrease as the length to width ratio increases. This implies that as we increase the thickness and allowable deflection improve the safety at the plate, whereas an increase in the span

(length) of the plate increases the failure tendency of the plate structure. It is also observed that the value of critical lateral load increase as the specified thickness (t) of plate increases, and decrease as the length to width ratio increases. This implies that as the

thickness is increased, the allowable deflection improves the safety of the plate, whereas an increase in the span (length) of the plate increases the failure tendency of the isotropic rectangular CCFS plate structure.

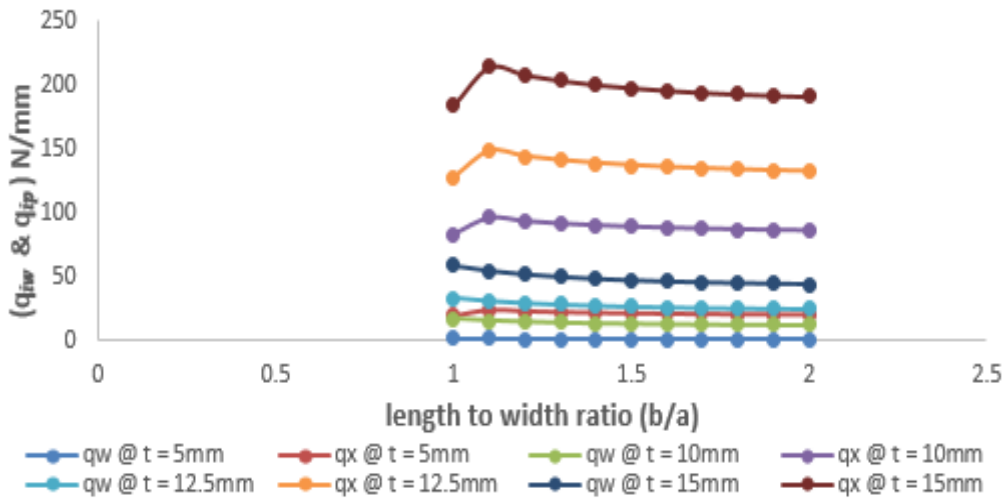


**Fig. 6** Graph of critical load versus length to width ratio of CCFS plate for span, a = 3.0 m at  $w_a = 3.0$  mm.

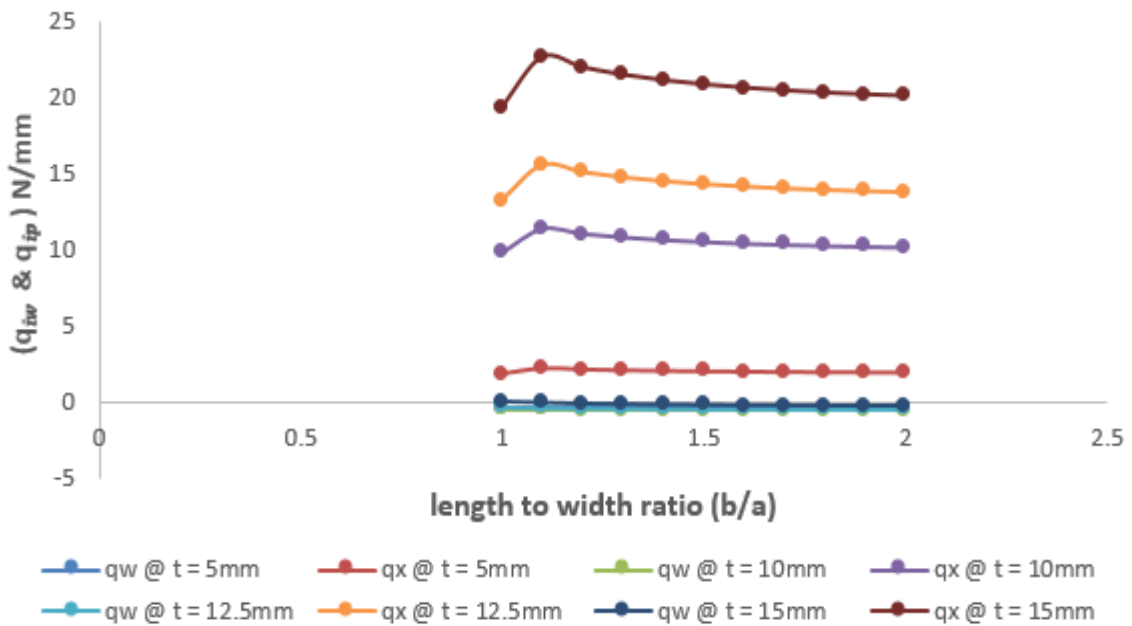


**Fig. 7** Graph of critical load versus length to width ratio of CCFS plate for span, a = 3.0 m at  $w_a = 5.0$  mm.



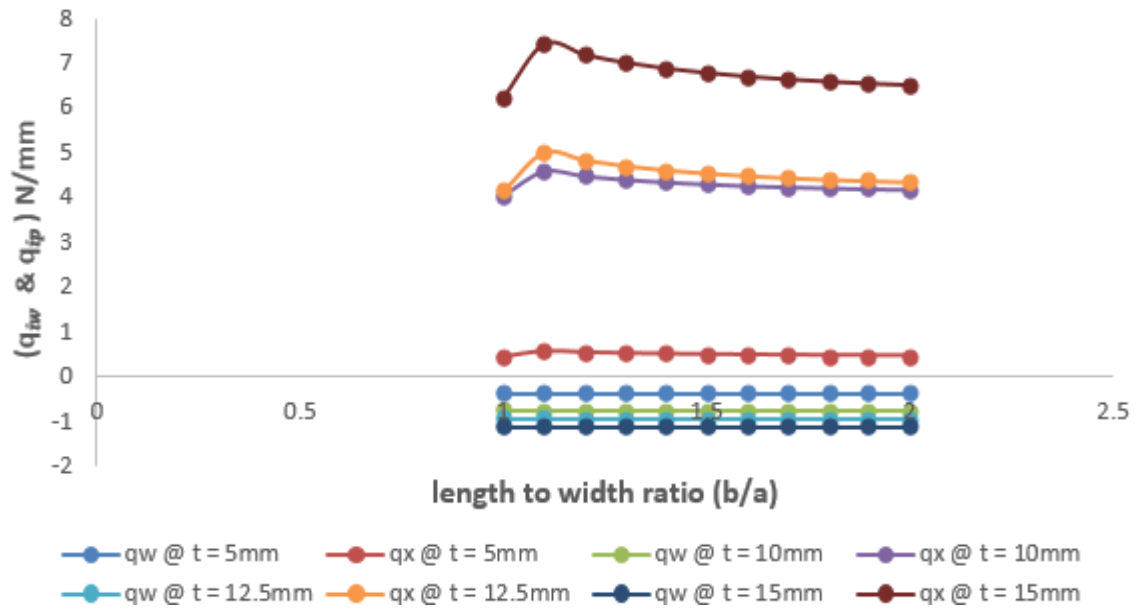


**Fig. 8** Graph of critical load versus length to width ratio of CCFS plate for span,  $a = 5.0$  m at  $w_a = 1.0$  mm.

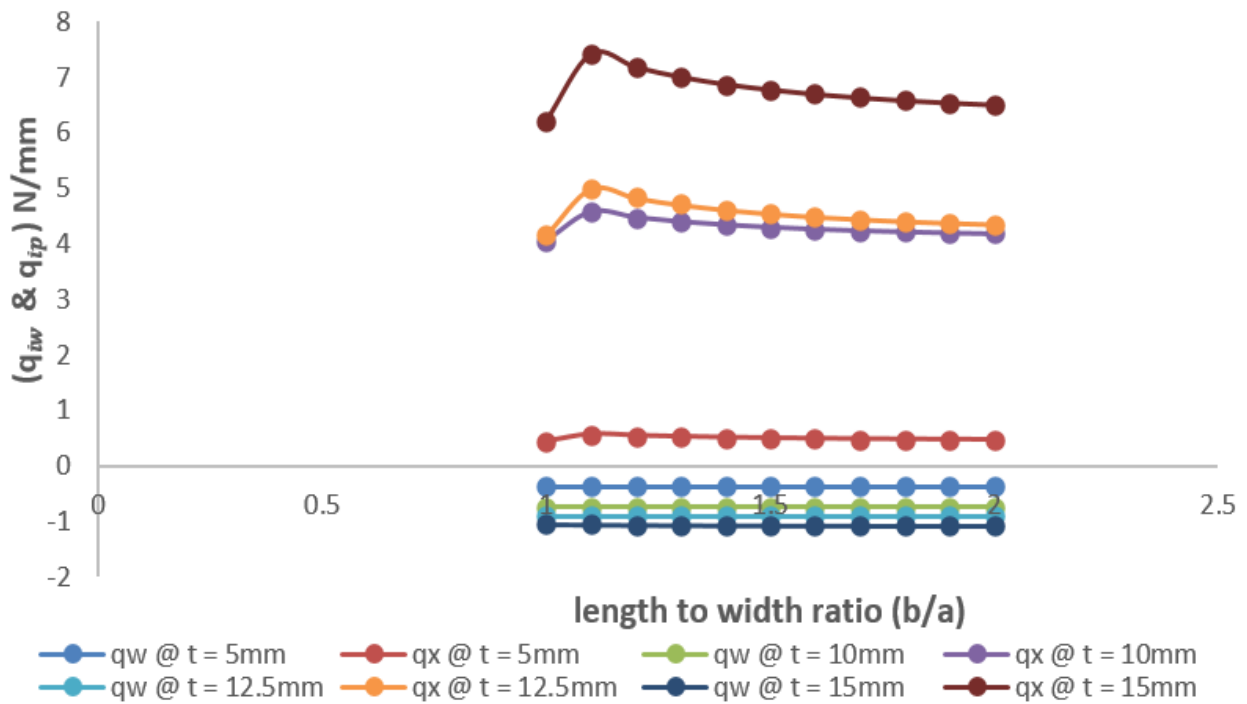


**Fig. 9** Graph of critical load versus length to width ratio of CCFS plate for span,  $a = 5000$  mm at  $w_a = 3.0$  mm.

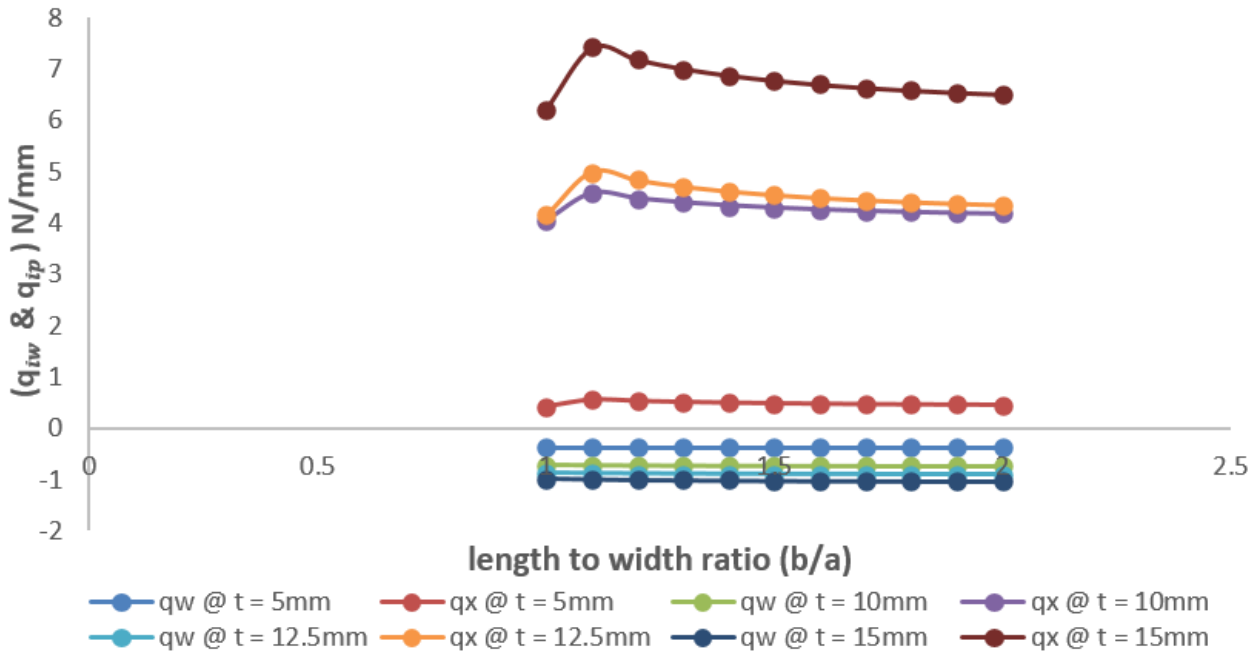


**Fig. 10** Graph of critical load versus length to width ratio of CCFS plate for span,  $a = 5.0$  m at  $w_a = 5.0$  mm.

#### 4. Conclusion

Based on the result of the analysis, the following conclusions are made:

- the theory considered shear deformation effect without shear correction factor inclusion;
- the constitutive relations used satisfied transverse shear stress variation while predicting the bending of CCFS thin and thick rectangular plate;
- critical lateral load increase as the thickness ( $t$ ) of plate increases;
- critical lateral load decrease as the length to width ratio increases;
- the value of  $q_{ip}$  if greater than that of  $q_{iw}$  can be said that the failure of plate in  $q_{iw}$  is like a warning requesting maintenance whereas failure in  $q_{ip}$  means total failure and cannot be maintained; and
- the failure in deflection ( $q_{iw}$ ) is seen in the CCFS plate but failure in shear ( $q_{ip}$ ), which leads to crack is not seen in all the aspect ratio in consideration.

#### Conflict of Interests

The authors declare that there is no conflict of interests regarding the publication of this paper.

#### ORCID

Festus C. Onyeka <https://orcid.org/0000-0002-2668-9753>

Thompson E. Okeke <https://orcid.org/0000-0003-4743-5055>

#### References

- R. Li, P. Wang, Y. Tian, B. Wang, and G. Li. "A unified analytic solution approach to static bending and free vibration problems of rectangular thin plates," *Sci. Rep.*, vol. 5, 17054, 2015, doi: 10.1038/srep17054
- F. C. Onyeka, "Direct analysis of critical lateral load in a thick rectangular plate using refined plate theory," *Int. J. Civ. Eng. Technol.*, vol. 10, no. 5, pp. 492-505, 2019.
- R. B. Pipes, and N. J. Pagano, "Interlinear stresses in composite laminates under axial extension," *J. Compos. Mater.*, vol. 4, pp. 538-648, 1970.
- A. S. Mantari, C. Oktem, and G. Soares, "A new trigonometric shear deformation theory for isotropic, laminated composite and sandwich plates," *Int. J. Solids Struct.*, vol. 49, pp. 43-53, 2012.
- R. D. Mindlin, "Influence of rotary inertia and shear on flexural motions of isotropic, elastic plates," *ASME J. Appl. Mech.*, vol. 18, pp. 31-38, 1951.
- G. R. Kirchhoff, "About the balance and the movement of an elastic disk," *J. Pure Appl. Maths*, vol. 40, pp. 51-88, 1850.
- G. R. Kirchhoff, "About the vibrations of a circular elastic disc," *Ann. Phys. Chem.*, vol. 81, pp. 258-264, 1850.
- Y. M. Ghugal, and A. S. Sayyad, "Free vibration of thick isotropic plates using trigonometric shear deformation theory," *J. Solid Mech.*, vol. 3, no. 2, pp. 172-182, 2011.
- A. S. Sayyad, and Y. M. Ghugal, "Bending and free vibration analysis of thick isotropic plates by using exponential shear deformation

- theory," *Appl. Comput. Mech.*, vol. 6, 2, pp. 65–82, 2012.
- [10] A. S. Sayyad, and Y. M. Ghugal, "Buckling analysis of thick isotropic plates by using exponential shear deformation theory," *Appl. Comput. Mech.*, vol. 6, no. 2, pp. 185–192, 2012.
- [11] K. P. Soldatos, "On certain refined theories for plate bending," *ASME J. Appl. Mech.*, vol. 55, pp. 994–995, 1988.
- [12] A. Mahi, E-A. Bedia, and A. Tausi, "A new hyperbolic shear deformation theory for bending and free vibration analysis of an isotropic functionally graded, sandwich, laminated composite plate," *Appl. Math. Model.*, vol. 25, 2489-2508, 2015.
- [13] O. M. Ibearugbulem, and F. C. Onyeka, "Moment and stress analysis solutions of clamped rectangular thick plate," *Eur. J. Eng. Res. Sci.*, vol. 5, no. 4, pp. 531-534, 2020.
- [14] F. C. Onyeka, and O. M. Ibearugbulem, "Load analysis and bending solutions of rectangular thick plate," *Int. J. Emerg. Technol.*, vol. 11, no. 3, pp. 1103–1110, 2020.